Using Synchrophasors for Controlled Islanding—A Prospective Application for the Uruguayan Power System

Ricardo Franco, *Member, IEEE*, Celia Sena, Glauco N. Taranto, *Senior Member, IEEE*, and Alvaro Giusto

***Abstract*—This paper describes two wide-area protection schemes for controlled islanding of the Uruguayan electrical power system. The first scheme relies only on local signals available for distance protection relays, whereas the second scheme is based both on local and remote synchrophasor measurements. The paper compares results in terms of load shedding amount necessary to maintain system integrity, with and without the proposed protection schemes. The investigation is based on comprehensive transient stability studies using actual dynamical models. Past occurrences that led the system to widespread blackouts have motivated the investigations presented in this paper.**

***Index Terms*—Controlled islanding, dynamic simulation, out-of-step protection, PMU, synchrophasors, transient stability, WAMPAC.**

I. Introduction

CONTROLLED islanding in electric power networks must be fast, precise and reliable, since it normally deals with significant structural changes in the network [1], [2]. This paper describes two wide-area protection (WAP) schemes for controlled islanding in the Uruguayan power system. The first scheme relies only on local signals available for distance protection relays, and the second scheme is based on local and remote synchrophasor measurements [3], [4].

Uruguay is facing strong energetic challenges. The traditional arrange, dominated by hydro and oil-based thermal generation backed up by international AC interconnections, is being confronted by the growth of the demand, the fuel prices, and a worsening of the hydro scenario. The responses to this panorama are the ongoing plans of energetic expansion and diversification that specify, among others, the appearance of various, geographically-distributed private-owned small generators and wind-farms. The new scenarios have been object of studies reported in [5] and [6].

The Uruguayan power system can be described as two large areas. Bulk generation comes mainly from the hydro units located in the North and Center (hereafter namely North), while the largest consumer center and the main thermal units are located in the South. Fig. 1 depicts a schematic diagram of the network. The North and South areas are interconnected by two 500-kV lines (Palmar-Montevideo circuits shown in red dashed lines) and a set of 150-kV lines (blue dashed lines) connecting Montevideo to other regions.

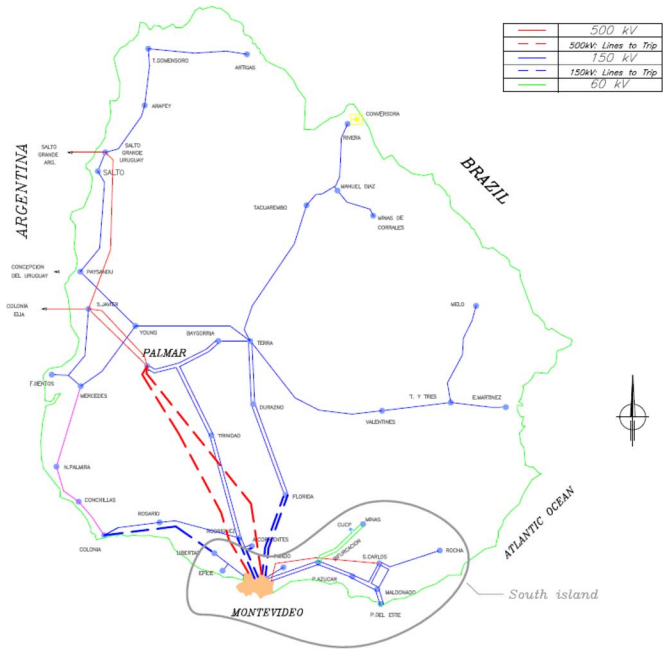

Fig. 1. Uruguayan power system.

The main characteristics of the Uruguayan power system can be summarized with the following numbers:

- peak demand (winter 2010): 1.7 GW;
- installed generation: 2.6 GW (1.4 hydro + 1.2 thermal);
- transmission system: 1,000 km @ 500 kV and 3560 km @ 150 kV;
- strong AC interconnection with Argentina 2 GVA @ 500 kV – 50 Hz in the West, and a small-capacity (70 MW) HVDC interconnection with Brazil in the East.

Disturbances that cause the outage of both 500-kV lines Palmar-Montevideo lead the system to a widespread blackout including the critical area of great Montevideo, where 80% of the country's demand is located. In order to minimize the load curtailment caused by this severe outage, this paper investigates the controlled separation of the system into two stable islands, the minimum amount of necessary load shedding in

Manuscript received April 27, 2012; revised September 05, 2012; accepted October 06, 2012. Date of publication November 19, 2012; date of current version April 18, 2013. Paper no. TPWRS-00423-2012.

R. Franco and C. Sena are with UTE, the National Electric Utility of Uruguay, and also with the Universidad de la República, Montevideo, Uruguay (e-mail: rfranco@ute.com.uy; celiam.sena@gmail.com).

G. N. Taranto is with the Federal University of Rio de Janeiro, COPPE/UFRJ, 21945-970 Rio de Janeiro, Brazil (e-mail: tarang@coep.ufrj.br).

A. Giusto is with the Universidad de la República, Montevideo, Uruguay (e-mail: alvaro@fing.edu.uy).

Color versions of one or more of the figures in this paper are available online at http://ieeexplore.ieee.org.

Digital Object Identifier 10.1109/TPWRS.2012.2224142

the importing area, and in what time those actions should take place.

To assess these questions, the paper compares two proposed WAP schemes against the current protection strategy implemented on field.

The first WAP scheme is based on conventional power swing blocking (PSB) and out-of-step tripping (OST) functions included in distance protection relays, namely PSB-OST scheme [7], [8]. The controlled islanding was performed by measuring, locally, the rate of change of the impedance at both ends of 150-kV lines. This strategy acts at four pre-selected 150-kV locations to make the North-South separation. The OST function was complemented with PSB function installed in other locations to prevent undesirable relay operations and network separation. Further details of this protective scheme are included in [9].

The second WAP scheme utilizes a novel algorithm based on synchrophasors called predictive out-of-step tripping, namely OOST scheme proposed in [10]–[15]. The detection of unstable oscillations is based on voltage phasors that are measured at both ends of the 500-kV lines. The instability is identified by monitoring slip (rate of change of their relative phase) and acceleration (rate of change of slip). Many oscillation patterns in the slip-acceleration plane were synthesized in order to assess the detection and prediction performance of the OOST algorithm.

A comprehensive set of simulations is performed using the complete and official database of the Uruguayan network by transient stability analysis along with a simplified model of the neighbor Argentinian network [16].

The main contribution of this paper is the comparative analysis of the results obtained with two different wide-area protective strategies (one based on distance relays, and the other based on synchrophasors) to detect the system separation after a severe fault. The analysis is based on simulations of a detailed dynamical model of the Uruguayan system. The results are also compared to the current protective strategy used by the utility.

The paper is organized as follows: Section II focuses on the out-of-step theory for line distance protection, and Section III describes the synchrophasor theory for WAP. The simulations and studies performed are described in Section IV, including a discussion of the protection strategies, and Section V wraps up the paper with some concluding remarks.

II. Distance Protection and Power System Stability

There are many technical books and papers describing power system stability and its relation to distance protection [7], [8], [17]. Electromechanical oscillations are common events in power systems. They may be the consequence of any disturbance in the power system such as line switching, faults, load shedding and generator tripping. During normal operation the magnitude of the oscillations are usually small and damped, but during abnormal operation the oscillations can become sustainable or undamped.

The loss of synchronism between areas affects the transmission lines relays. Distance relay elements may operate during a power swing, if the impedance locus enters the distance operating characteristic.

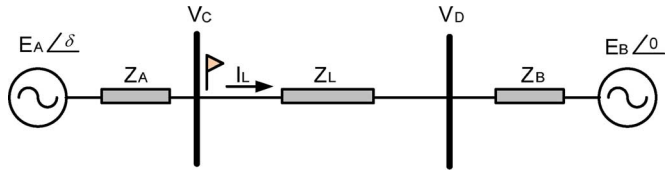

Fig. 2. Two-machine system.

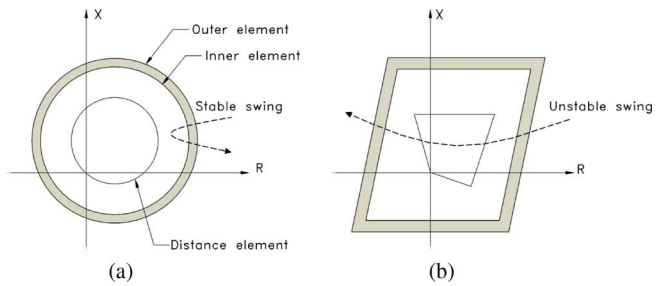

Fig. 3. Circular and quadrilateral power swing detection characteristic.

A. Distance Relays

Distance relays respond to positive-sequence quantities. The impedance measured by the distance relay during a power swing depends on the phase angle separation (δ) between the two equivalent system source voltages.

The two-machine equivalent system shown in Fig. 2 can be used to describe the performance of distance protection during electromechanical power swings. The impedance seen by the relay at point C during a power swing can be determined by (1), when assuming equal magnitude for the voltage sources, i.e., $|\mathrm{E\_A}| = |\mathrm{E\_B}| = 1$ p.u.:

$$Z_C = \frac{V_C}{I_L} = \frac{(Z_A + Z_B + Z_L)}{2}\left(1 - j\cot\frac{\delta}{2}\right) - Z_A. \quad (1)$$

During a power swing the angle δ varies. For stable swing, the angle δ increases to a maximum value when the trajectory shifts direction and δ decreases to a minimum value, from where the trajectory shifts direction again. This sequence repeats until the power swing ends. For unstable swing, the δ trajectory reaches 180°.

B. Power Swing Detection Methods

The traditional and most commonly used method in power swing detection is based on measuring the positive-sequence impedance and the transition time through a blocking impedance area in the R-X diagram, as shown in Fig. 3. The movement of the impedance for short circuit faults is faster compared to the movement of a power swing.

A timer starts when the measured impedance enters the outer layer. If the measured impedance remains between the inner and outer layers for the set time delay, it is considered a power swing and the tripping of the relay is blocked during a certain period of time (Fig. 3). However, if the impedance crosses the inner and outer layers in a time shorter than the set time delay, the disturbance is considered a short circuit and tripping is allowed.

C. Out-of-Step Protection Functions

In order to prevent cascading failures triggered by the loss of synchronism, it is common the application of out-of-step protec-

tion functions. These functions detect the out-of-step conditions and take actions to separate affected areas, minimizing the loss of load and maintaining the service continuity.

There are two functions related to out-of-step detection. One is the OST function that discriminates between stable and unstable power swings, and starts a network islanding during loss of synchronism. The other is the PSB function that discriminates between a fault and a power swing. This function blocks the relay elements that are prepared to operate.

D. Out-of-Step Tripping (OST) and Power Swing Blocking (PSB) Functions

The OST schemes are planned to protect the power system during unstable power swings, isolating unstable generators or subsystems by the formation of stable islands. These functions must be installed in some pre-selected locations, and network separation must take place at these locations. The OST scheme must be supplemented with a PSB function installed in other locations, to prevent undesirable relay operations and network separation in an indiscriminate way.

The combination of OST and PSB functions for the controlled separation of the Uruguayan system into two stable islands, namely Strategy #1, is described later in Section IV.

III. Out-of-Step and Unstable Power Swings Detection With Synchrophasors

Synchrophasors can effectively be used to detect out-of-step or unstable power swings and are the basis of modern WAP schemes. Three algorithms based on synchrophasors are described in this section, to be later combined and applied to the Uruguayan power system.

Synchrophasors are defined as phasors calculated from a sampled voltage or current measurement, using a common or standard time signal [3]. A synchrophasor is represented as a complex number. Its module is the rms value of the magnitude and its argument is the instantaneous phase angle at nominal system frequency synchronized to universal time coordinated (UTC) [18].

A phasor measurement unit (PMU) is a device that measures one- or three-phase AC electrical variables according to the general definition and accuracy required in the IEEE Synchrophasor Standard C37.118.1-2011 [19].

The standard IEEE C37.118-2005 [20] did not address the synchrophasors accuracy and time response under transient conditions; therefore, all tests were restricted to steady-state conditions. However, modern PMUs designed and constructed under that standard are capable of making accurate measurements under transient conditions, and there have been many publications documenting this feature [18]. The present technology allows the use of synchrophasors to measure power swings in power systems. New IEEE C37.118.1-2011 [19] standard includes dynamic requirements besides steady state, so static and dynamic interoperability of different manufacturers' PMUs is possible.

Time synchronization with Global Positioning System (GPS) and IRIG-B or IEEE 1588 time dissemination is enough to achieve 1 μs accuracy or better, that corresponds to a 0.018° angle error or to a total vector error (TVE) of 0.031%.

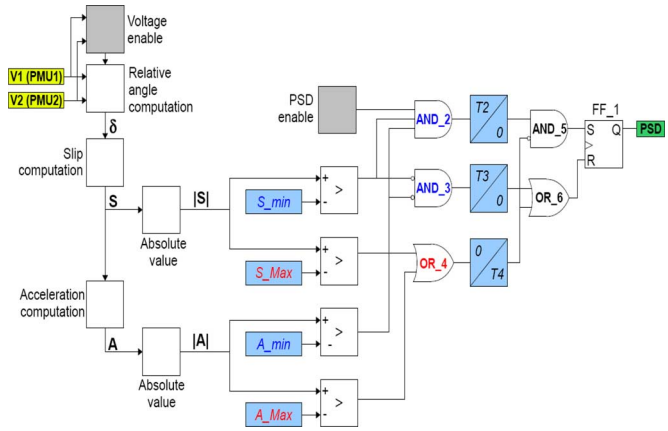

Fig. 4. PSD diagram.

Adequate communication capability is needed to send synchrophasors data to the phasor data concentrator (PDC) in order to process them and take decisions.

A. Detection of Unstable Power Swing With Synchrophasors, PSD, and OOST Algorithms

Power swing detection (PSD) and predictive out-of-step tripping (OOST) algorithms patented by Guzman-Casillas and Schweitzer Engineering Laboratories, Inc. (SEL) [10], [11] are based on synchrophasors. These algorithms were studied comprehensively, slightly modified and suitably combined to test their prospective application in the Uruguayan power system for WAP protection and controlled islanding.

The distinctive characteristic of these algorithms is the use of the second derivative $\ddot{\delta}$ (acceleration, A, in Hz/sec) and the first derivative $\dot{\delta}$ (velocity or slip, S, in Hz) of the synchronized phase angle difference between two nodal voltages. These quantities are computed from subsequent samples of the relative angle δ:

$$\dot{\delta}_i = \frac{1}{360}\frac{\delta_i - \delta_{i-1}}{t_i - t_{i-1}} \quad [Hz] \tag{2}$$

$$\ddot{\delta}_i = \frac{\dot{\delta}_i - \dot{\delta}_{i-1}}{t_i - t_{i-1}} \quad \left[\frac{Hz}{s}\right]. \tag{3}$$

The placement of the two PMUs must ensure that the electrical center is between them. The PSD algorithm has the block diagram shown in Fig. 4 and it is described referring to Fig. 5, which represents the $A - S$ plane. In few words, the PSD function is cleared (to a "False" value) when the trajectory in the $A - S$ plane enters the regions labeled "*RESET*" in Fig. 5, i.e., when A and S are both small or both large with respect to suitably chosen threshold values.

PSD is set to "True" value when the trajectory enters the regions labelled "SET", where both variables A and S show intermediate values. When the trajectory enters in any of the white regions in Fig. 5, the PSD function is not modified and its last value is retained. Each transition has a timer associated in order to avoid spurious detections.

OOST algorithm is also based on the A-S plane and can be described with the help of Fig. 6. The algorithm identifies as unstable any trajectory going out of the central strip.

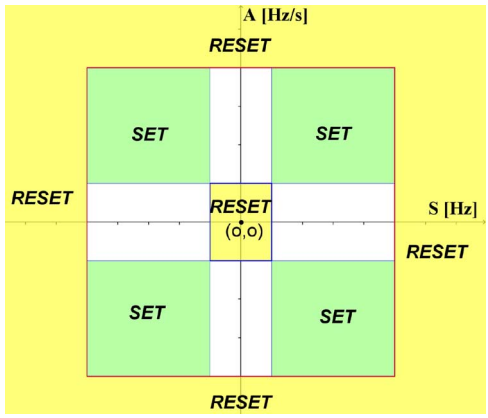

Fig. 5. PSD characteristic on the A-S plane.

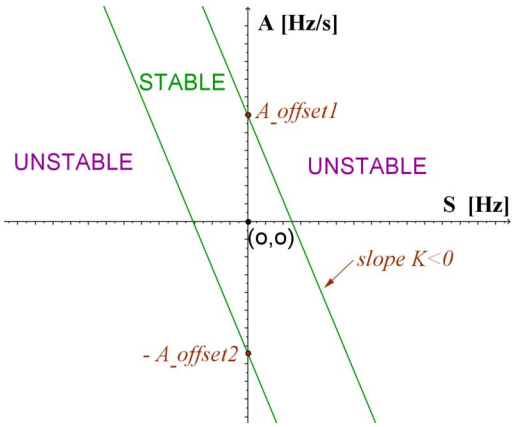

Fig. 6. OOST characteristic on the A-S plane.

The idea behind this zone can be briefly described as follows. A monotonous unstable trajectory will go outside of the stable strip either by right or left since the slip variation direction will be unchanged. An unstable oscillatory trajectory will appear as a growing spiral hitting the boundaries after some cycles. A detailed discussion about the interpretation of the trajectories in the $A-S$ plane is included in Section III-B. The corresponding logical block diagram is shown in Fig. 7. Transitions have also timers associated.

Both algorithms PSD and OOST have a predictive behavior, since the detection is not only based on the angle, but also on its first and second derivative. A detailed study of different oscillation patterns in the A-S plane was performed in [21] along with a discussion of the role of each algorithm. Complementary to these approaches is the algorithm out-of-step detection (OOSD) [10] which is only based on the angle. A slightly modified variant of this algorithm, named OOSDv, is shown in Fig. 8. It basically consists in the comparison of the absolute value of the angle with a suitable threshold (typically 120 degrees to detect out-of-step condition [21]). The same behavior can be obtained by a proper configuration of applications in patent [20].

The out-of-step condition and the unstable swings are assessed with the combination of the three functions PSD, OOST, and OOSDv in the following way:

The combined OOST and PSD characteristic of Fig. 9 may be seen as the superposition of Figs. 5 and 6. The characteristic

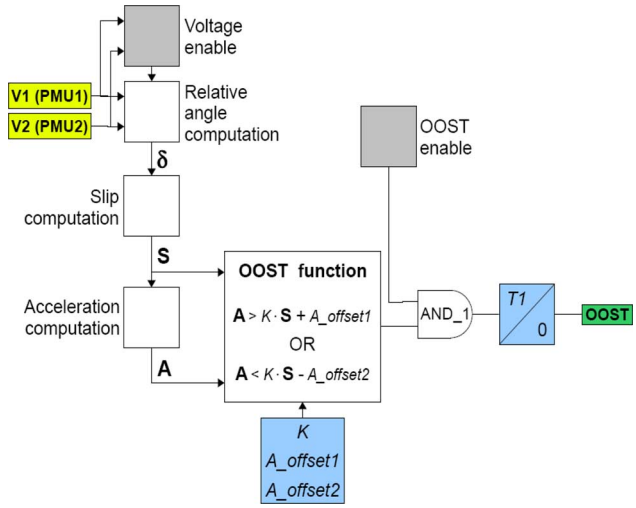

Fig. 7. OOST block diagram.

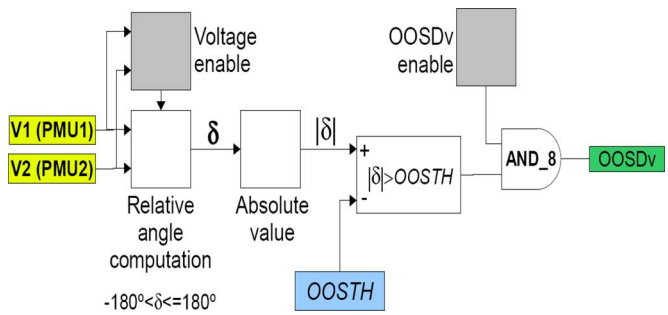

Fig. 8. OOSDv block diagram.

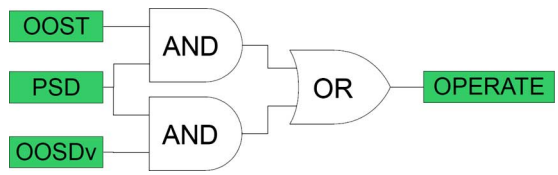

Fig. 9. Logical function on OOST, PSD, and OOSDv.

TABLE I
PSD-OOST PARAMETERS

S_min = 0.09 Hz	*T2* = 3 cycles	*A_offset1* = 2.1 Hz/s
S_Max = 10 Hz	*T3* = 3 cycles	*A_offset2* = 2.6 Hz/s
A_min = 0.1 Hz/s	*T4* = 3 cycles	*T1* = 3 cycles
A_Max = 40 Hz/s	*K* = - 2.4 s^{-1}	*OOSTH* = 120°

is shown, with the parameters of Table I of Section IV, on the A-S plane as seen in Fig. 10.

As A_min and S_min are very small, see Table I, the inner yellow reset region and the white regions of Fig. 5 are imperceptible in Fig. 10.

In the presence of detected power swings (PSD function), the WAP scheme is operated if either predictive or conventional out-of-step is detected (OOST, OOSDv). This procedure was used for the studies developed for the Uruguayan network in Strategy#2 described in Section IV.

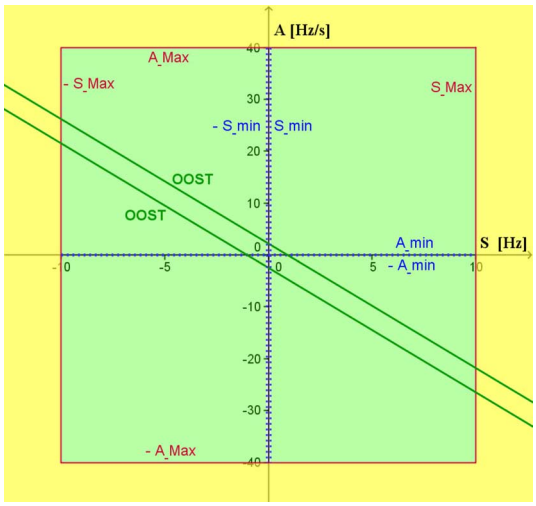

Fig. 10. OOST and PSD characteristic on the A-S plane.

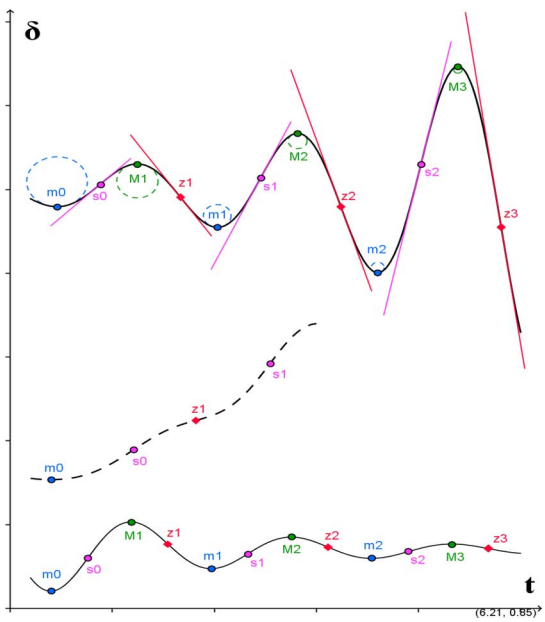

Fig. 11. Representative $\delta(t)$ time responses.

B. Quantitative Analysis of Transient Response in the A-S Plane

Transient behavior of power systems is studied with the help of different plots. Angular time responses are commonly visualized in $\delta(t)$, $\dot{\delta}(t)$ plots. The protection systems typically are studied on the impedance $R-X$ plane. Each analysis tool provides meaningful information once the patterns associated to the basic phenomena under study are known.

The predictive algorithms described in Section III-A take decisions based on the location of the trajectories on the $A-S$ plane. This analysis tool is not thoroughly exploited in the power system literature, but it has its roots on the well-known phase-plane plots, used in the classical literature of dynamical systems [23].

Fig. 11 shows three typical time responses, commonly found in transient stability studies where a representative relative angle is plotted as a function of time. An unstable oscillatory response is shown in the upper plot, along with a non-oscillatory unstable response (center plot) and a stable damped response (lower plot).

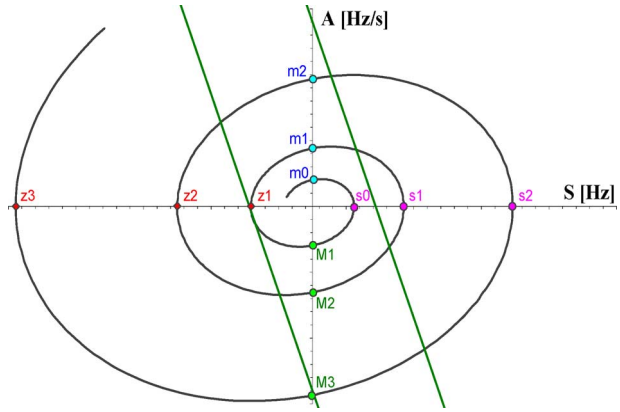

Fig. 12. A-S plot of oscillatory unstable trajectory.

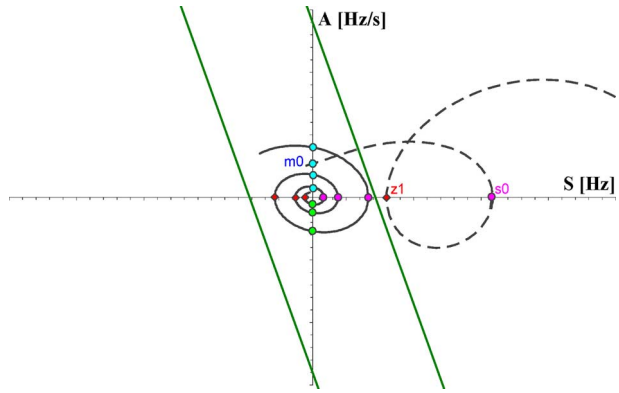

Fig. 13. A-S plots of time responses of Fig. 11.

Consider the upper plot of Fig. 11. Characteristic singular points are marked, namely the local maxima (M_i), minima (m_i), the inflection points with positive (s_i) and negative (z_i) derivative. The osculating circles, for the maxima and minima, are also shown. The second derivatives at these points are inversely proportional to the respective radii. The corresponding plot in the $A-S$ plane is shown in Fig. 12.

Growing swings result in a growing spiral linking the positive and negative inflection points on the abscissa axis and the maxima and minima on the ordinate axis. Fig. 13 shows the $A-S$ plots of the two remaining time responses in Fig. 11.

The dashed line in Fig. 13 (that corresponds to the dashed center plot of Fig. 11) has a characteristic loop of out-of-step or loss of synchronism that crosses the abscissa axis without encircling the origin. So, the OOST algorithm appears predictive or preventive since the out-of-step is detected by OOST when the trajectory goes outside of the central stable strip (green lines) and before the mentioned loop occurs.

The PSD function described with the help of Fig. 5 can be briefly explained as follows. In steady-state condition, power systems ideally operate at the origin (0,0) of the A-S plane. Normal operation moves slightly the point around the origin and motivates the central RESET region marked yellow in the

figure. On the other hand, excessive acceleration or slip are associated to short circuits and motivate the outer RESET yellow region.

IV. Time Domain Dynamical Simulations

The Uruguayan power network model used in this study contains approximately 360 buses and nearly 50 generator units. Most of these units are hydroelectrical generators. The neighbor Argentinian network is represented by a reduced model with three equivalent generators, referred to as "Ezeiza", "Almafuerte" and "Rodríguez", and detailed models for the hydroelectrical generator units at "Yaciretá" and "Salto Grande" [16]. The Uruguayan power system model includes the complete power grids of 500 kV and 150 kV and part of the 60-kV grid. Fifth-order and 6th-order models are utilized for the hydro and thermal synchronous machines, respectively.

The scenario under study is one with maximum thermal generation with some hydro units in service. The scenario assumes that one of the 500-kV Palmar-Montevideo lines is out of service. The critical contingency is a fault in the remaining 500-kV line that carries power from North to South.

The disturbance to be analyzed is the following:

1) A 3-phase fault at $\mathrm{t} = 1$ s, on the mentioned 500-kV line, near the Montevideo end.
2) The clearance times used were:
   a) $\mathrm{t} = 60$ ms (3 cycles) for the near end
   b) $\mathrm{t} = 80$ ms (4 cycles) for the far end
3) The fault is removed with the complete outage of the line.

After the fault is removed, the power system is divided into two groups of coherent machines: one that presents a frequency over the nominal (50 Hz); and the other that presents a frequency under the nominal. The respective over and under frequency simply reflects the mismatch between load and generation for each subsystem.

Three emergency protection strategies involving load shedding in the South and network separation are analyzed and compared:

1) Strategy#0—mimics utility current practice, which consists of a large amount of load shedding with no network separation;
2) Strategy#1—performs load shedding and network separation into two stable islands, considering only local measurements;
3) Strategy#2—also performs load shedding and network separation, but considers both local and remote synchronized phasors.

This investigation was performed with the software DSATools [24]. The action of the protective devices on the network was not automated into DSATools. Instead, the tripping actions were thoroughly studied in A-S plots using DSATools outputs and Matlab [25], successively.

A. Strategy#0—Load Shedding

This strategy, the one actually in operation, consists in a load shedding on the subsystem that presented low frequency, in order to maintain the whole network connected through the 150-kV lines. So, after the removal of the fault, 600 MVA of load was rejected in Montevideo's area, representing 36% of the total load in the Uruguayan system.

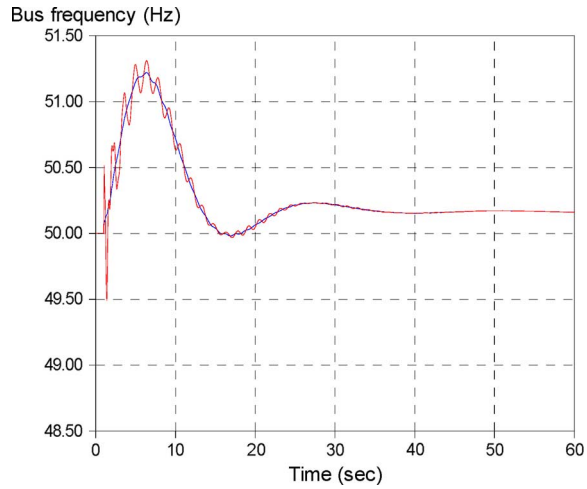

Fig. 14. System frequencies with Strategy#0.

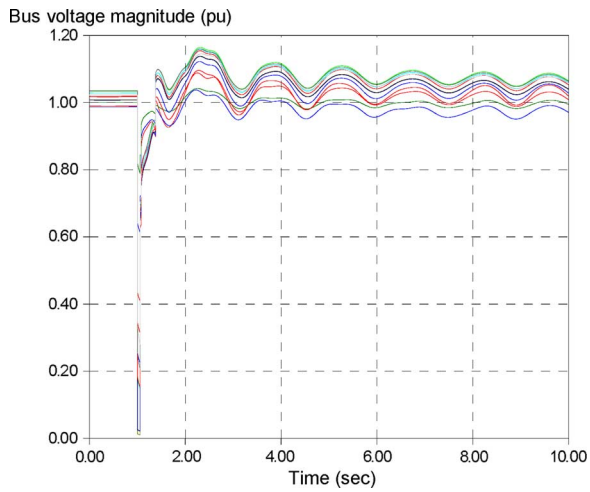

Fig. 15. System voltages with Strategy#0.

The impacts of the load shedding on frequency and voltages are shown in Figs. 14 and 15, respectively.

We remark the significance of the amount of the load shed. The critical results shown in Strategy#0 motivated the investigation of alternative emergency protective schemes, that would consider controlled network separation.

The UFLS scheme is based on under-frequency relays installed in substations, in order to trip the low-voltage circuit breakers. The low-frequency setting is 49.5 Hz, instantaneous tripping [9].

B. Strategy#1—Controlled Islanding and Load Shedding With Local Measurement

The islanding scheme must be applied to pre-selected network locations, preferably near the electrical center, and network separation must take place at such locations to preserve a close balance between load and generation. The island scheme can be performed by installing OST functions in the preselected locations.

In the Uruguayan network, the electrical center is located in the middle of Montevideo city, which makes difficult the suitable splitting of the system. Thus, the locations to perform the

islanding were changed to the southern ends of the 150-kV lines linking Montevideo with the North. The resulting South island is formed by the busbars within the circled area shown in Fig. 1. Therefore, 300 ms after the fault was cleared, the power system splits in two islands. To perform a controlled islanding, the PSB function must be installed in some lines to avoid uncontrolled trip of some lines. The time is selected to allow the protection system to detect the North-South low-frequency oscillation (250 ms), let the breakers open (50 ms) and minimize the number out-of-step functions to install.

Since the controlled islanding was performed in four points relatively far from the electrical center, both islands were unbalanced in load and generation. A load shedding scheme was implemented at the South island. The amount of load shed was 496 MW. The load shedding was set to be done 300 ms after the island formation. The time selection criterion for the load shedding is dependent on the under frequency protection limit: 48.5 Hz. The load shedding must occurs before the under frequency relays trip the generating units in the South island. The impact of this protective strategy on frequency is shown in Fig. 16; the voltages (not shown) have a behavior similar to Fig. 15.

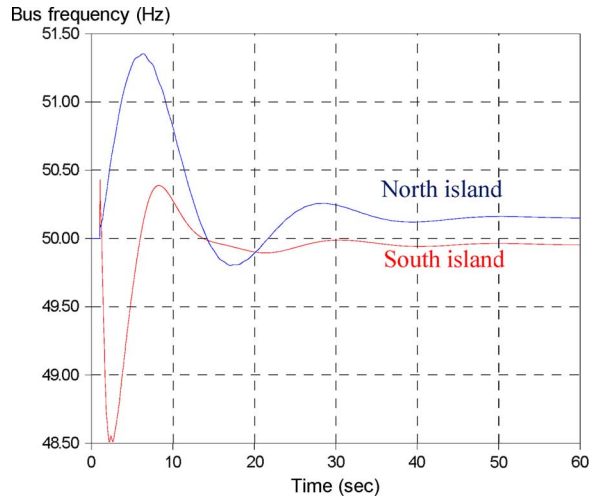

Fig. 16. North (blue) and South (red) frequencies with Strategy#1.

C. Strategy#2—Controlled Islanding and Load Shedding With Synchrophasor

This strategy uses the function OPERATE that results of the logical combination of functions PSD, OOST and OOSDv shown in Figs. 9 and 10. The case under study is the same already described for Strategy#1. The same contingency, the same sites for tripping, and the same places for load shedding are used. Likewise it was done for Strategy#1, a comprehensive set of contingencies and operating scenarios was also analyzed to evaluate the PSD-OOST algorithm performance and to establish a robust arrangement for its settings, shown in Table I.

The procedure to establish these settings was based on simulations and the direct experience with the system under study. The analysis started with typical values proposed in [10]–[15] but without timers. Then acceleration, slip and slope settings were modified until OOST and PSD worked suitably. Finally, all the settings, timers included, were adjusted interactively to their definitive values. This procedure was carried out for a representative set of scenarios and contingencies; see [21].

The two PMUs are simulated as located in Palmar (North) and Montevideo (South). With reference to Fig. 1, one of the two dashed 500-kV lines linking Montevideo and Palmar is initially out of service and the fault occurs on the other line. So, the bulk 500-kV link is suddenly lost, making the two strong 500-kV buses fall apart, thus becoming a natural choice for the PMU locations. We remark that the choice of the PMU locations is specific for the studied contingencies.

The PDC that receives synchrophasors data and performs the predictive PSD and OOST algorithms is simulated in Matlab [25].

The results show that the combination of PSD and OOST algorithms with the settings given in Table I detected South-North separation at 190 ms after the fault is cleared. This allows us to conclude that the islanding in 150 kV and load shedding can be done 250 ms after the fault is cleared.

Figs. 18 and 19 show the performance of the algorithms in the $A-S$ plane, as well as in the slip-phase plane, respectively,

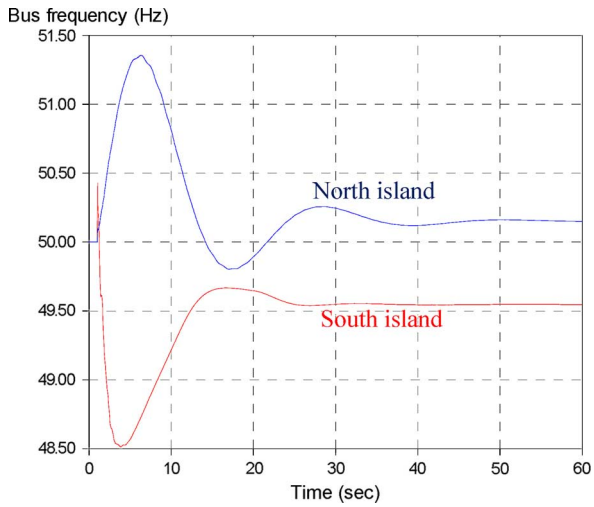

Fig. 17. North (blue) and South (red) frequencies with Strategy#2.

while Fig. 20 shows the time response of the angle difference of the 500-kV nodal voltages for the contingency under study. "O" is the stable pre-fault operating point, shown in the three plots. Red crosses represent points where PSD AND OOST function detects the 500-kV North-South separation, circumstance that triggers islanding by the opening of the 150-kV lines and performs the load shedding.

Fig. 18 shows the first out-of-step detection in a predictive way (first red cross, point B) once the T2 timer is completed after $\dot{\delta} = K \times \dot{\delta} + A\_offset1$ (upper green line) is exceeded in point A. Points D and F show the second and third out-of-step detection done by (OOST AND PSD) signal that sets the OPERATE signal of Fig. 9, and points C and E correspond to the reset of OOST signal. It is clear that only the first and faster out-of-step detection has practical interest; the others show the behavior of OOST algorithm.

Fig. 20 shows the angle trajectory, highlighting the same points A to F along with the logical signals (OOST AND PSD), (OOSDv AND PSD) and OPERATE defined in Fig. 9. It is also shown, with a blue dash-dotted line, the $\mathrm{OOSTH} = 120°$ setting of the OOSDv algoritm. It is seen that OOST function

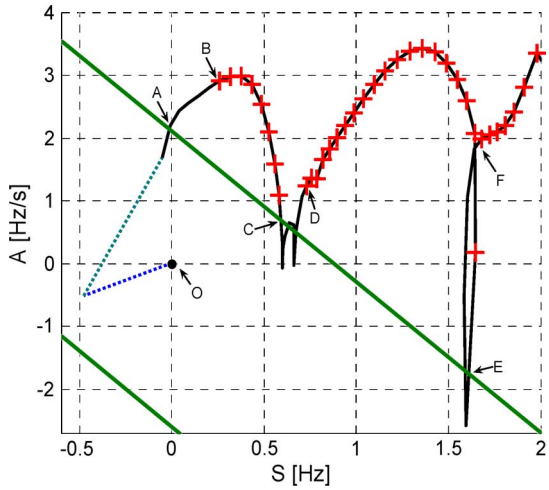

Fig. 18. Operation of combination of PSD and OOST algorithms on the $A-S$ plane.

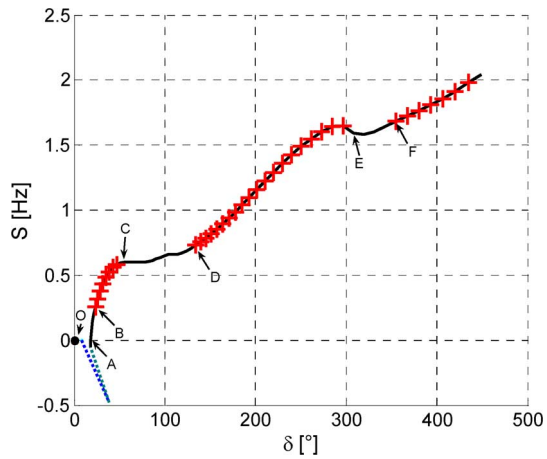

Fig. 19. Operation of PSD and OOST on the $S \times \delta$ plane.

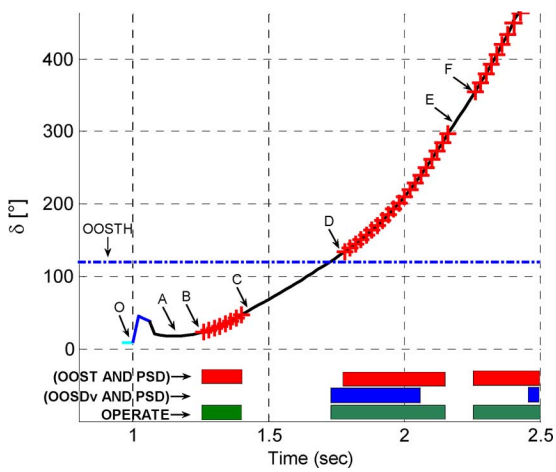

Fig. 20. Operation of PSD and OOST on the δ time response.

is faster than OOSDv function, even if a smaller OOSTH setting is used. So OOSDv is not relevant in this particular contingency.

Fig. 17 shows that the power system protected with Strategy#2 has frequency behavior similar to the Strategy#1 shown in Fig. 16. The South frequency for Strategy#2 has slower recovery with less overshoot and less final frequency. The voltage behavior, not shown, is also similar to Fig. 15.

TABLE II
LOAD SHEDDING

Strategy #0	Strategy #1	Strategy #2
602 MW	496 MW	418 MW
100%	82,40%	69,50%

The contingency under study is so critical that only a significant load shedding is able to prevent a widespread blackout. If the system is not split (Strategy#0), the minimum amount of the load shedding, able to keep acceptable transient behavior of the generation units is near 602 MW. This strategy has the advantage of keeping the system intact, but it has the biggest cost in terms of avoidable load shedding. Strategy#1 consists of the splitting at four preselected locations plus a load shedding allowing a stable operation in two islands with acceptable transient swings. The amount of load to be shed is 496 MW.

On the other hand, the use of synchrophasors for a predictive out-of-step detection, Strategy #2, has allowed a faster detection than Strategy #1. Thus, it turns possible a further reduction of the load shedding to 418 MW, ensuring the transient stability of both resulting islands. Table II summarizes the amount of load shedding, in percentage and absolute values, needed in each strategy analyzed.

V. CONCLUSIONS

This paper presented two WAP schemes for controlled islanding of the Uruguayan electrical power system. The performance of both approaches was assessed for different scenarios of generation and load profiles. The results showed that controlled islanding of the North-South tie with fast load shedding with both schemes performed significantly better than the current utility practice. The necessary load shedding was reduced by 18% when the PSB-OST scheme (using only local signals) was utilized, and by 30% when the OOST scheme (using synchrophasor measurement) was utilized when compared with the current utility practice. The OOST scheme looked more attractive since it is able to curtail less amount of load, due to its predictive capability. However, the PSB-OST scheme should not be discarded since it provides a simple and cost effective solution to the problem. It also has the advantage that it can be implemented with the current protection system already in place.

ACKNOWLEDGMENT

The authors would like to thank G. Casaravilla and C. Briozzo for providing the means of our collaboration. The authors also would like to thank UdelaR and CAPES for the financial support.

REFERENCES

[1] CIGRE Task Force 38.02.19, System Protection Schemes in Power Networks, Technical Brochure 187, Jun. 2001.

[2] B. Yang, V. Vittal, and G. T. Heydt, "Slow-coherency-based controlled islanding—A demonstration of the approach on the August 14, 2003 blackout scenario," *IEEE Trans. Power Syst.*, vol. 21, no. 4, pp. 1840–1847, Nov. 2006.

[3] A. G. Phadke, "Synchronized phasor measurements in power systems," *IEEE Comput. Appl. Power*, vol. 6, no. 2, pp. 10–15, Apr. 1993.
[4] A. G. Phadke and J. S. Thorp, *Synchronized Phasor Measurements and Their Applications*. New York: Springer, 2008.
[5] C. Sena, R. Franco, and A. Giusto, "Performance evaluation of power swing blocking functions and islanding protection—A case study on the Uruguayan network," in *Proc. IEEE PES General Meeting*, Jul. 2010.
[6] A. Giusto and P. Monzón, "Modal analysis of the Uruguayan electrical power system," in *Proc. IEEE PES General Meeting*, Jul. 2010.
[7] D. Tziovaras and D. Hou, "Out-of-step protection fundamentals and advancements," in *Proc. 30th Annu. Western Protective Relay Conf.*, Spokane, WA, Oct. 21–23, 2003.
[8] G. Benmouyal, D. Tziovaras, and D. Hou, "Zero-setting power-swing blocking protection," in *Proc. 31th Annu. Western Protective Relay Conf.*, Spokane, WA, Oct. 19–21, 2004.
[9] C. Sena, G. Taranto, and A. Giusto, "An investigation of controlled power system separation of the Uruguayan network," in *Proc. 2010 IREP Symp.—Bulk Power System Dynamics and Control*, Aug. 2010.
[10] A. Guzman-Casillas, "Systems and methods for power swing and out-of-step detection using time stamped data," International Application Published Under The Patent Cooperation Treaty (PCT), World Intellectual Property Organization International Bureau, International Publication Number WO 20091042966 Al, Apr. 2009.
[11] A. Guzman-Casillas, "Systems and methods for power swing and out-of-step detection using time stamped data," United States Patent Application Publication US 2009/0089608 A1, Apr. 2009.
[12] A. Guzman-Casillas, V. Mynam, and G. Zweigle, Schweitzer Engineering Laboratories, Inc., "Backup transmission line protection for ground faults and power swing detection using synchrophasors," Schweitzer Engineering Laboratories, Inc. 20070918, TP6291-01, 2007.
[13] E. Schweitzer, III, D. Whitehead, A. Guzman-Casillas, Y. Gong, and M. Donolo, "Advanced real-time synchrophasor applications," Schweitzer Engineering Laboratories, Inc. 20080923, TP6337-01, 2008.
[14] E. Schweitzer, III, A. Guzman-Casillas, H. Altuve, and D. Tziouvaras, "Real-time synchrophasor applications for wide-area protection, control, monitoring," Schweitzer Engineering Laboratories, Inc. 20090831, TP6379-01, 2009.
[15] E. Schweitzer, III, D. Whitehead, G. Zweigle, and K. Ravikumar, "Synchrophasor-based power system protection and control applications," in *Proc. Texas A&M Conf. Protective Relay Engineers*, 2010, IEEE, 20100304, TP6372-01.
[16] M. Artenstein and A. Giusto, "Equivalent models of the Argentinian electrical power system for stability analysis of the Uruguayan network," in *Proc. IEEE/PES Transmission and Distribution Conf. Expo.: Latin America, Colombia*, Aug. 2008.
[17] P. Kundur, *Power System Stability and Control*, ser. The EPRI Power System Engineering Series. New York: Mc-Graw-Hill, 1994.
[18] North American SynchroPhasor Initiative (NASPI), Performance and Standards Task Team (PSTT), Basic PMU Specification and Standard Definition, May 2008. [Online]. Available: https://www.naspi.org/site/Module/Resource/PMUInstallation.aspx.
[19] IEEE Standard, IEEE C37.118.1-2011 for Synchrophasor Measurements for Power Systems, Dec. 2011.
[20] IEEE Standard, IEEE C37.118-2005 for Synchrophasors for Power Systems, Mar. 2006.
[21] R. Franco, "Uso de Sincrofasores para la Detección de Oscilaciones de Potencia y Pérdida de Sincronismo. Aplicación al Sistema Eléctrico Uruguayo para la Separación Controlada en Islas," (in Spanish) M.Sc. thesis, Universidad de la República, Montevideo, Uruguay, 2012, ISSN: 1688-2806, ISSN: 1688-2792.
[22] A. Guzman-Casillas, M. Mynam, and M. Donolo, "Islanding Detection in an Electrical Power Delivery System," United States Patent Application Publication US 2010/0286838 A1, Nov. 2010.
[23] H. Khalil, *Nonlinear Systems*. Englewood Cliffs, NJ: Prentice Hall, 1996.
[24] DSATools—Dynamic Security Assessment Software, Powertech Labs Inc. [Online]. Available: http://www.powertechlabs.com.
[25] MATLAB—The Language of Technical Computing, The MathWorks Inc. [Online]. Available: http://www.mathworks.com.

Ricardo Franco (S'95–M'12) was born in Montevideo, Uruguay, in 1962. He received the Electrical Engineering degree from the Universidad de la República, Montevideo, in 1994. He is pursuing the master degree in electrical engineering.

He has worked in the Protection Section of Transmission (and Generation) of UTE (Uruguayan national electricity generation, transmission, and distribution public utility) since 1989. He has been with the Instituto de Ingeniería Eléctrica, Facultad de Ingeniería, Universidad de la República since 2007. His research interests are power system protection and relaying, WAMPAC, power system stability, and artificial neural networks.

Mr. Franco has been a CIGRÉ Member since 2008.

Celia Sena received the engineering degree in 1997 and the master degree in 2010 from Universidad de la República, Montevideo, Uruguay, both in electrical engineering.

Since 1992, she has been working at the public Uruguayan utility (UTE) at the Power System Protection Department. Since 2007, she has been with the Instituto de Ingeniería Eléctrica, Facultad de Ingeniería, Universidad de la República. Her research interests include power system protection, dynamics, and control.

Glauco N. Taranto (S'92–M'96–SM'04) received the B.Sc. degree in 1988 from the State University of Rio de Janeiro, Rio de Janeiro, Brazil, the M.Sc. degree in 1991 from the Catholic University of Rio de Janeiro, and the Ph.D. degree in 1994 from Rensselaer Polytechnic Institute, Troy, NY, all in electrical engineering.

In 2006, he was on sabbatical leave as a Visiting Fellow at CESI, Milan, Italy. Since 1995, he has been with the Electrical Engineering Department, Federal University of Rio de Janeiro/COPPE, Brazil, where he is currently an Associate Professor. His research interests include power system dynamics and controls, intelligent control, and robust control design.

Dr. Taranto is a member of the IEEE PES, PSDP Committee, IEEE CSS, and CIGRÉ.

Alvaro Giusto was born in Montevideo, Uruguay, in 1965. He received the Electrical Engineering degree in 1992 and the Ph.D. Degree in 2010 from the Universidad de la República, Montevideo, Uruguay, and the M.Sc. degree from the Universidade Federal de Santa Catarina, Brazil.

He has been with the Instituto de Ingeniería Eléctrica, Facultad de Ingeniería, Universidad de la República since 1990. He has been working as an independent consultant in automation and control since 1998. His research interests are power system stability, control theory, and control applications.